

Efficient generation of axial magnetic field by multiple laser beams with twisted pointing directions

Yin Shi¹, Alexey Arefiev², Jue Xuan Hao¹, and Jian Zheng^{1,3}

¹Department of Plasma Physics and Fusion Engineering,
University of Science and Technology of China, Hefei 230026, China

²Department of Mechanical and Aerospace Engineering,
University of California at San Diego, La Jolla, CA 92093, USA

³Collaborative Innovation Center of IFSA,
Shanghai Jiao Tong University, Shanghai 200240, Peoples Republic of China

22nd March 2023

Abstract

Strong laser-driven magnetic fields are crucial for high-energy-density physics and laboratory astrophysics research, but generation of axial multi-kT fields remains a challenge. The difficulty comes from the inability of a conventional linearly polarized laser beam to induce the required azimuthal current or, equivalently, angular momentum (AM). We show that several laser beams can overcome this difficulty. Our three-dimensional kinetic simulations demonstrate that a twist in their pointing directions enables them to carry orbital AM and transfer it to the plasma, thus generating a hot electron population carrying AM needed to sustain the magnetic field. The resulting multi-kT field occupies a volume that is tens of thousands of cubic microns and it persists on a ps time scale. The mechanism can be realized for a wide range of laser intensities and pulse durations. Our scheme is well-suited for implementation using multi-kJ PW-class lasers, because, by design, they have multiple beamlets and because the scheme requires only linear-polarization.

Recently, magnetic field effects in high energy density physics (HEDP) have attracted significant interest [1, 2, 3]. These can range from guiding of relativistic electron beams [4] to affecting the shape of inertial fusion implosions [5]. Despite significant progress, generation of sufficiently strong and controllable macroscopic fields at the laser facilities used for HEDP research [6, 7, 8, 9, 10, 11] remains an outstanding challenge.

Various approaches to magnetic field generation using high-power lasers have been explored in search of an optimal mechanism and field configuration. Initial efforts were focused on leveraging a circularly polarized (CP) laser beam to generate an axial quasi-static plasma magnetic field [12, 13, 14]. The emergence of capabilities to create Laguerre-Gaussian (LG) high-intensity beams has stimulated research into generation of the axial field using such beams as well [15, 16, 17, 18]. The strength of the plasma field is limited by the laser's ability to drive a strong azimuthal current, so it is insightful to interpret the process as a transfer of the laser's angular momentum \mathbf{L} to the plasma. Here $\mathbf{L} = \varepsilon_0 \int \mathbf{r} \times [\mathbf{E} \times \mathbf{B}] d^3\mathbf{r}$, where ε_0 is the dielectric permittivity, \mathbf{E} and \mathbf{B} are the electric and magnetic fields, respectively.

Setups involving conventional linearly polarized

(LP) laser beams have also received attention, because additional optics is required to make CP or LG beams from the conventional beams. A large-scale uniform magnetic fields can be created by a ns laser irradiating a capacitor-coil [3, 19, 20, 21] or a snail target [22]. This field can then be amplified inside a plasma by a high intensity ps or sub-ps laser pulse [23, 24, 25, 26]. Relativistic electrons generated by high-intensity laser pulses can also generate surface or bulk azimuthal magnetic fields when streaming through a solid density target [27, 28, 29, 30], and these fields are beneficial for hot electron transport and electron beam collimation [13, 14, 31, 32, 33, 34, 35, 36]. Applications for longitudinal fields include guiding of relativistic electron beams [37, 3, 19], laser-driven ion acceleration [38, 39], magnetized atomic physics [40, 3], and laboratory astrophysics [41].

Generation of a large-volume strong magnetic field requires significant energy that must be delivered by the laser. Multi-kJ PW-class laser systems like LFEX [9], NIF ARC [10], and Petal [11] offer the highest energy that can be delivered on a ps time scale. These lasers are all composed of multiple LP beamlets. The multi-beamlet configuration is not just an essential feature of the laser system design,

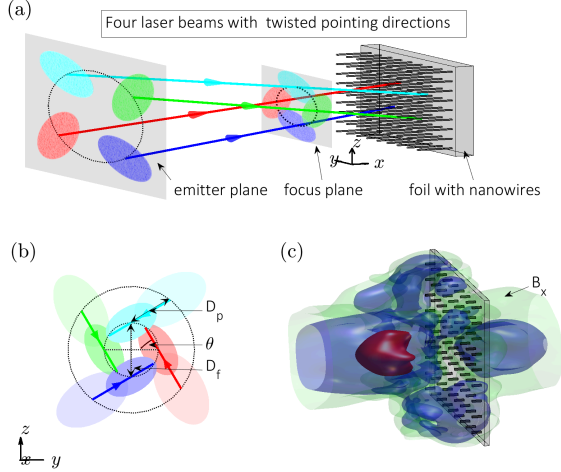


Figure 1: (a) Setup for axial magnetic field generation using four linearly-polarized Gaussian laser beams with twisted pointing directions, shown with solid lines, and a structured target. The size of each beam is shown with a color-coded ellipse in the emitter plane (left side of the simulation box) and in the focus plane. (b) Projections of the two planes on to the (y, z) -plane. The parameters setting up the beam orientation are defined in the text. (c) Surface plots of the axial magnetic field B_x after the lasers have left the simulation box ($t = 20$ fs). The green, blue, and red surfaces represent $B_x/B_0 = -0.1, -0.2,$ and -0.8 , where $B_0 = 13.4$ kT.

but also the key to advanced laser-plasma interaction regimes [42]. The number of multi-beamlet facilities will increase, as SG-II UP [8] is due to be upgraded to have multiple kJ-class ps laser beams.

This Letter presents a new multi-beam approach for efficient laser-to-plasma angular momentum (AM) transfer resulting in magnetic field generation. The approach, illustrated in Fig. 1 for four linearly-polarized Gaussian beams, is motivated by the capability of multi-kJ PW-class laser systems to provide multiple beamlets [9, 10, 43, 11]. Our scheme eliminates the need for CP or LG beams while offering a method for generating a field above 10 kT in a $10^4 \mu\text{m}^3$ volume. Our scheme provides a plasma that can potentially be used for studies of astrophysical objects involving strong magnetic fields beyond the dynamic range of previous laboratory settings [44, 45] and to mimic a rotating plasma environment in astrophysics [46, 47].

The role of the twist in the pointing direction, Fig. 1(a), can be illustrated using geometrical optics. Each laser beam is represented by a ray directed along the wave vector \mathbf{k}_i , where i is the index numbering the beam. The photon momentum in the i -th beam is $\mathbf{p}_i = \hbar\mathbf{k}_i$. Consider a pair of tilted rays, $\mathbf{k}_{1,2} = (k_x, k_\perp^{(1,2)}, 0)$, that intersect the (y, z) -plane at

$z_{1,2} = \pm D_f/2$ and $y_{1,2} = 0$, where $D_f/2$ is the beam offset. The axial AM of a photon is $[\mathbf{r} \times \mathbf{p}]_x$, so the total AM of the two beams is $L_x \approx -N\hbar(k_\perp^1 - k_\perp^2)D_f/2$, where N is the number of photons in each beam. The AM can be doubled by adding two rays offset in y . The rays appear twisted, so it is appropriate to refer to the calculated AM as orbital angular momentum (OAM). They carry OAM, a distinct form of AM, even though each beam has no intrinsic AM [48]. There are parallels to γ -ray beams carrying OAM [49, 50, 51] composed of photons with a twisted distribution of \mathbf{p} .

To investigate the transfer of the OAM carried by four laser beams, we have performed a series of three-dimensional (3D) particle-in-cell (PIC) simulations using a relativistic PIC code EPOCH [52]. Each beam is a linearly polarized Gaussian beam. The duration of each pulse is 450 fs and the peak intensity is $2.1 \times 10^{20} \text{ Wcm}^{-2}$. Our target is a flat foil with sub-wavelength diameter nanowires whose purpose is to increase the interaction volume between the laser beams and the plasma produced by the target and thus enhances the number of hot electrons [53]. The front and rear surfaces of the foil are located at $x_{f1} = 0 \mu\text{m}$ and $x_{f2} = 4 \mu\text{m}$. The spacing between the wires is $2 \mu\text{m}$, the wire length is $5 \mu\text{m}$, and the wire width is $0.4 \mu\text{m}$. The entire target is initialized as a fully ionized cold carbon plasma with an electron density of $50n_c$, where $n_c = 1.8 \times 10^{21} \text{ cm}^{-3}$ is the critical density corresponding to a laser wavelength $\lambda = 0.8 \mu\text{m}$. All simulation parameters are listed in the Supplemental Material.

The orientation of the four beams is set according to Fig. 1. Their axes intersect a given plane perpendicular to the x -axis with the intersection points forming vertices of a square. We use two planes: the emitter plane ($x_e = -20 \mu\text{m}$), which is the left boundary of the simulation box, and the focus plane ($x_f = -16 \mu\text{m}$), which is the plane where the beams have the smallest transverse size. The twist is set by angle θ . There is no twist for $\theta = 0$, so that the axis of each beam and the x -axis form a plane. We use $\phi = \arctan(-D_p/S)$ to set the beam convergence, where S is the distance between the emitter plane and the focus plane and D_p is the transverse shift of the beam axes between the two planes, as shown in Fig. 1(b). We use $\phi = -0.27\pi$ in all simulations.

Figure 1(c) shows the magnetic field (B-field) for $\theta = -0.28\pi$ at $t = 20$ fs. We define $t = 0$ fs as the time when the laser pulses leave the simulation box. The laser-plasma interaction takes place at $t \in (-510, -60)$ fs. The longitudinal B-field exceeds 10 kT. The volume is around $10^4 \mu\text{m}^3$. The three surfaces show $B_x/B_0 = -0.1, -0.2,$ and -0.8 , where $B_0 = 13.4$ kT. Note that $B_0 \equiv 2\pi m_e c/|e|\lambda_L$, where $\lambda_L = 0.8 \mu\text{m}$ is laser wavelength in vacuum, c is the speed of light, and e and m_e are the electron charge

and mass. To make its profile more clear, B_x is averaged temporally over a 20 fs interval and spatially using a box with stencil size $0.4 \mu\text{m} \times 0.4 \mu\text{m} \times 0.4 \mu\text{m}$.

Owing to the approximately axisymmetric profile of B_x , we can examine its 2D distributions in Fig. 2 without missing too much information. Figure 2(a) shows the global distribution in the (x, y) -plane. The nanowires are between $x_{wire} = -5 \mu\text{m}$ and $x_{f1} = 0 \mu\text{m}$. The foil is between $x_{f1} = 0 \mu\text{m}$ and $x_{f2} = 4 \mu\text{m}$. Figures 2(b)&(c) show B_x , averaged over the azimuthal angle, as a function of x and r in front of and behind the target (note the different color-scale ranges). We find that $|B_x|$ can be as high as $1.5B_0$ in front of the wires because the lasers generate a higher concentration of hot electrons in front of the foil. Reaching this amplitude is noteworthy because new phenomena of laser beam transport through a plasma can arise at $|B_x| \gtrsim B_0$ [54, 55]. Even though B_x is weaker behind the target, it is in the range of kT. This confirms that our scheme indeed produces electrons carrying AM, as the lasers are unable to reach behind the target to generate the B-field locally.

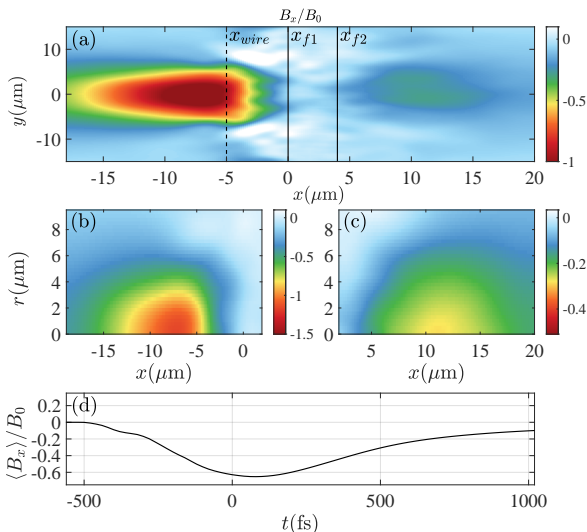


Figure 2: (a) Axial magnetic field in the (x, y) -plane at $t = 20$ fs. (b)&(c) Angle-averaged axial magnetic field as a function of x and r at $t = 20$ fs. The nanowire region is at $x_{wire} < x < x_{f1}$. The foil is at $x_{f1} \leq x \leq x_{f2}$. (d) Time evolution of the volume-averaged magnetic field within a box with $-15 \mu\text{m} < x < x_{wire}$, $|y| < 5 \mu\text{m}$, and $|z| < 5 \mu\text{m}$.

Figure 2(d) shows the time evolution of the average magnetic field strength $\langle B_x \rangle$ in a box with $-15 \mu\text{m} < x < -5 \mu\text{m}$, $|y| < 5 \mu\text{m}$, and $|z| < 5 \mu\text{m}$. The ps time scale is comparable to that in Ref. [56], but the region containing the magnetic field moves axially outward (away from the target). In terms of the energy content within a region with $|y|, |z| < 15 \mu\text{m}$, we find that the energy in the magnetic

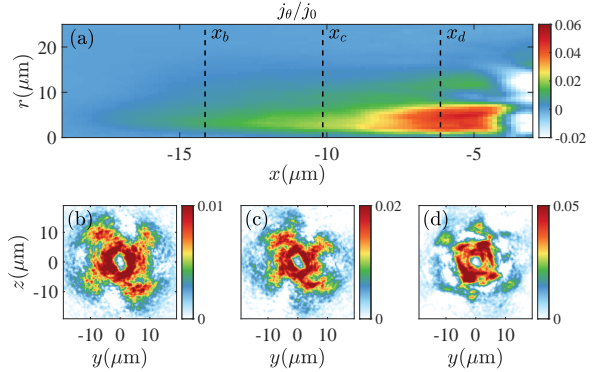


Figure 3: (a) Angle-averaged azimuthal current density j_θ at $t = 20$ fs as a function of x and r . (b), (c), and (d) j_θ in the (y, z) -plane at three different locations with $x = x_b, x_c,$ and x_d . Note the significant difference in color-scales between the three panels introduced to improve visibility. The current density is normalized to $j_0 = -|e|cn_c = -8.25 \times 10^{16} \text{ A/m}^2$.

field ($\varepsilon_B = \int B_x^2 / (2\mu_0) dV \approx 3.0 \text{ J}$) is much smaller than the kinetic energy of electrons ($\varepsilon_e \approx 40.0 \text{ J}$). The energy of the four beams is $\varepsilon_{laser} \approx 580 \text{ J}$. The energy conversion efficiency from laser to hot electrons and from hot electrons to the magnetic field are both around 10%. The overall conversion efficiency is two orders of magnitude higher than that for a laser-driven coil in Ref. [2].

To confirm that the twist angle θ rather than the polarization is the key parameter, we performed a simulation without the twist ($\theta = 0$) and a simulation with an opposite twist to the original direction ($\theta = 0.28\pi$). We found that no axial magnetic field is generated without the twist and that B_x reverses its direction when we reverse the twist. The azimuthal B-field is generated in all three cases due to the ubiquitous axial current driven by the laser pulses. We also performed a simulation with the original setup but randomly selected direction of the E-field polarization in each laser beam. The angle-averaged B_x is similar to the B_x in Fig. 2, confirming that laser polarization has only a secondary effect on the magnetic field generation in our setup.

In the remainder of this letter we focus on the region in front of the target. We start with an analysis of the azimuthal current density j_θ that is thought to be responsible for the axial magnetic field generation. Figure 3(a) shows j_θ , averaged over the azimuthal angle, in the (x, r) -plane at $t = 20$ fs. The direction of j_θ alternates in the nanowire region [$x \in (-5, 0) \mu\text{m}$]. The underlying cause is the presence of strong nonuniformities in the ion density associated with the original nanowires.

Transverse distributions of j_θ in the (y, z) -plane at different x positions (x_b, x_c, x_d) are shown in Fig. 3(b-d). These positions are marked by dashed

lines in Fig. 3(a). In agreement with Fig. 3(a), $|j_\theta|$ is the biggest at x_d and the smallest at x_b . To perform an order of magnitude estimation for the maximum value of $|B_x|$, we assume that j_θ is uniform inside a cylinder of radius R and length Δx . Then the Biot-Savart law [57] yields

$$\begin{aligned} \max |B_x| &\approx \frac{\mu_0}{2} \int_0^R \int_{-\Delta x}^{\Delta x} \frac{|j_\theta| r^2 dx dr}{(r^2 + x^2)^{3/2}} \\ &= \mu_0 |j_\theta| \Delta x \operatorname{arsinh}(R/\Delta x), \end{aligned} \quad (1)$$

where $\mu_0 = 1.26 \times 10^{-6}$ H/m is permeability in vacuum. According to Fig. 3(a), we can set $R \approx \Delta x \approx 5 \mu\text{m}$. In Fig. 3(d), the current density reaches $|j_\theta| \approx 0.05|j_0|$, where $j_0 \equiv -|e|cn_c$. Using this value, we obtain $\max |B_x| \sim 20$ kT, which is close to the peak magnetic field, $B_x \sim 1.5B_0$, in Fig. 2(b).

To quantify the rotating effect of the plasma, we computed the density of the axial AM for electrons and ions. Due to the significant difference in mass, the ratio of the axial AM absorption between electrons and ions is $\eta_{ei} \approx 0.01$. We can estimate the AM density of hot electrons using the azimuthal current density. We write the AM density of electrons as $L_{xe} \approx r\gamma_a m_e n_e v_\theta$, where γ_a is the relativistic gamma-factor, n_e is the number density, and v_θ is the effective azimuthal velocity. We set $v_\theta \approx -j_\theta/|e|n_e$ to find that $L_{xe} \approx r\gamma_a m_e j_\theta/|e|$. For $r = w_0$ and $\gamma_a \approx \sqrt{1 + a_0^2} \approx 10$, we have $L_{xe} \approx 1.6$ kg/m-s. Using the electron density from simulations, $n_e \approx 10^{27} \text{ m}^{-3}$, we find that the rotating velocity is around $v_\theta \approx 0.1c$. Our setup produces a rotating plasma environment with electron density and rotation velocity two orders of magnitude higher than an LG beam in [16].

The OAM transfer from the laser beams to the electrons can be determined using the conservation of AM [12, 15, 56]. The OAM of absorbed laser photons is transferred to electrons and ions, with the electron fraction equal to η_{ei} . Then, based on the photon absorption, the axial AM density of the electrons is roughly

$$\begin{aligned} L_{ex}(x, r) &\approx \frac{\eta_{ei}}{x_\kappa} \frac{0.75\tau_g I_0}{c} \sin(\phi) \sin(\theta) D_{xr}, \\ D_{xr} &= r e^{x/x_\kappa - 2(r - D_f/2)^2/w_0^2}, \end{aligned} \quad (2)$$

where I_0 is the peak intensity of the incident laser pulses and τ_g is their duration. For simplicity, we assume that the absorption coefficient f_{abs} of the laser intensity over the axial distance is $f_{abs} = f_0 \exp(x/x_\kappa)$. We find from the simulation that $\eta = \int_{x=x_e}^{x=0} f_{abs} dx \approx x_\kappa f_0 \approx 0.1$ ($x_\kappa \approx 3 \mu\text{m}$). We use $r = D_f/2 = 6 \mu\text{m}$ and $x = 0 \mu\text{m}$ to find the peak AM density of the electrons, $L_{ex} \approx 2.4$ kg/m-s. This result is on the same scale as the peak AM density (≈ 6.9 kg/m-s) in our simulations. It is also close to the result (≈ 1.6 kg/m-s) calculated using j_θ in Fig. 3.

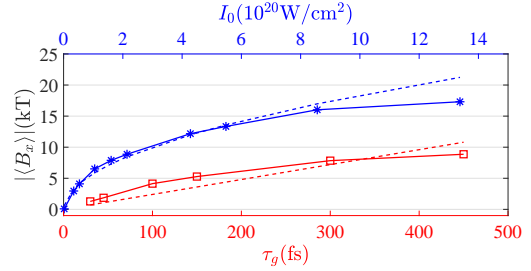


Figure 4: Volume-averaged magnetic field $\langle B_x \rangle$ as a function of peak laser intensity I_0 (blue asterisk markers) and laser pulse duration τ_g (red square markers). The averaging is performed within a box with $-15 \mu\text{m} < x < x_{wire}$, $|y| < 5 \mu\text{m}$, and $|z| < 5 \mu\text{m}$. The dashed curves (blue and red) show the fits based on Eq. (3).

The peak AM density in the simulation exceeds our model's prediction, which may be due to the locally positive AM density in the nanowire region. According to Eq. (2), the axial B-field can be controlled by changing the sign of twist angle θ , which has been confirmed in the Supplemental Material. Our model ignores the dependence of f_{abs} on such parameters like I_0 , ϕ , and θ , but the actual absorption mechanism may be more complex [58, 59, 60]. Using L_{ex} , we can obtain the azimuthal current density and the associated axial B-field,

$$B_x \propto \frac{j_\theta(x, r)}{j_0} \propto (\eta\eta_{ei}) \frac{a_0^2}{\gamma_a} \frac{c\tau_g}{x_\kappa} \frac{D_{xr}}{r} \sin(\phi) \sin(\theta). \quad (3)$$

To investigate the robustness of this mechanism to the choice of laser parameters, we perform scans over laser peak intensity I_0 and pulse duration τ_g . The dependence of the volume-averaged longitudinal field on I_0 , shown in Fig. 4 with asterisk markers, matches well the dependence given by Eq. (3) and shown with the blue dashed line. The blue dashed line is $\langle B_x \rangle [\text{kT}] = 0.85a_0^2/\sqrt{1+a_0^2}$. Even at $I_0 \approx 3 \times 10^{19} \text{ W/cm}^2$ ($a_0 = 4$), the axial magnetic field strength can be as high as 5 kT. The pulse duration scan, shown in Fig. 4 with square markers, is performed for a fixed peak intensity of $I_0 \approx 2.1 \times 10^{20} \text{ W/cm}^2$ ($a_0 = 10$). The red dashed line, $\langle B_x \rangle [\text{kT}] = 0.024\tau_g [\text{fs}]$, has the same dependence on τ_g as that given by Eq. (3). The laser pulse duration is believed to affect the number of hot electrons and, as a result, the magnetic field generation. For τ_g as small as 30 fs, we can still get a volume-averaged magnetic field of 1.3 kT. Additional simulations with a laser wavelength of $1.053 \mu\text{m}$ produce similar results, confirming that our scheme is applicable to both Ti:Sa and neodymium-based lasers.

In summary, we have demonstrated via 3D kinetic simulations a novel mechanism for generating a multi-kT axial magnetic field using multiple reg-

ular laser pulses. The twist in the pointing direction of the pulses is the key to driving an azimuthal plasma current that sustains the magnetic field. The twist angle is a convenient control knob for adjusting the direction and magnitude of the axial magnetic field. The field occupies a volume that is tens of thousands of cubic microns and it persists on a ps time scale. The mechanism can be realized for a wide range of laser intensities and pulse durations. Our scheme requires just regular linearly-polarized laser beams, which makes it suitable for implementation at existing and future multi-kJ PW-class laser facilities that, by design, have to have multiple beamlets [9, 10, 11, 42, 61], including the SG-II UP facility [8] that is expected to have multiple kJ-class ps pulses in the near future.

Acknowledgements

Y S acknowledges the support by USTC Research Funds of the Double First-Class Initiative, Strategic Priority Research Program of CAS (Grant No. XDA25010200), CAS Project for Young Scientists in Basic Research (Grant No. YSBR060) and Newton International Fellows Alumni follow-on funding. Y S also acknowledge Rui Yan and Robert Kingham for enthusiastic discussions. A. Arefiev's research was supported under the National Science Foundation–Czech Science Foundation partnership by NSF Award No. PHY-2206777. Simulations were performed with EPOCH (developed under UK EPSRC Grants EP/G054950/1, EP/G056803/1, EP/G055165/1, and EP/M022463/1). The computational center of USTC and Hefei Advanced Computing Center are acknowledged for computational support.

References

- [1] J. D. Moody, B. B. Pollock, H. Sio, D. J. Strozzi, D. D.-M. Ho, C. A. Walsh, G. E. Kemp, B. Lahmann, S. O. Kucheyev, B. Kozioziemski, E. G. Carroll, J. Kroll, D. K. Yanagisawa, J. Angus, B. Bachmann, S. D. Bhandarkar, J. D. Bude, L. Divol, B. Ferguson, J. Fry, L. Hagler, E. Hartouni, M. C. Herrmann, W. Hsing, D. M. Holunga, N. Izumi, J. Javedani, A. Johnson, S. Khan, D. Kalantar, T. Kohut, B. G. Logan, N. Masters, A. Nikroo, N. Orsi, K. Piston, C. Provencher, A. Rowe, J. Sater, K. Skulina, W. A. Stygar, V. Tang, S. E. Winters, G. Zimmerman, P. Adrian, J. P. Chittenden, B. Appelbe, A. Boxall, A. Crilly, S. O'Neill, J. Davies, J. Peebles, and S. Fujioka, "Increased ion temperature and neutron yield observed in magnetized indirectly driven d₂-filled capsule implosions on the national ignition facility," *Phys. Rev. Lett.*, vol. 129, p. 195002, Nov 2022.
- [2] G. Pérez-Callejo, C. Vlachos, C. A. Walsh, R. Florido, M. Bailly-Grandvaux, X. Vaisseau, F. Suzuki-Vidal, C. McGuffey, F. N. Beg, P. Bradford, V. Ospina-Bohórquez, D. Batani, D. Raffestin, A. Colaitis, V. Tikhonchuk, A. Casner, M. Koenig, B. Albertazzi, R. Fedosejevs, N. Woolsey, M. Ehret, A. Debayle, P. Loiseau, A. Calisti, S. Ferri, J. Honrubia, R. Kingham, R. C. Mancini, M. A. Gigosos, and J. J. Santos, "Cylindrical implosion platform for the study of highly magnetized plasmas at laser megajoule," *Phys. Rev. E*, vol. 106, p. 035206, Sep 2022.
- [3] J. J. Santos, M. Bailly-Grandvaux, M. Ehret, A. V. Arefiev, D. Batani, F. N. Beg, A. Calisti, S. Ferri, R. Florido, P. Forestier-Colleoni, S. Fujioka, M. A. Gigosos, L. Giuffrida, L. Gremillet, J. J. Honrubia, S. Kojima, P. Korneev, K. F. F. Law, J.-R. Marquès, A. Morace, C. Mossé, O. Peyrusse, S. Rose, M. Roth, S. Sakata, G. Schaumann, F. Suzuki-Vidal, V. T. Tikhonchuk, T. Toncian, N. Woolsey, and Z. Zhang, "Laser-driven strong magnetostatic fields with applications to charged beam transport and magnetized high energy-density physics," *Physics of Plasmas*, vol. 25, no. 5, p. 056705, 2018.
- [4] M. Bailly-Grandvaux, J. J. Santos, C. Bellei, P. Forestier-Colleoni, S. Fujioka, L. Giuffrida, J. J. Honrubia, D. Batani, R. Bouillaud, M. Chevrot, J. E. Cross, R. Crowston, S. Dorard, J.-L. Dubois, M. Ehret, G. Gregori, S. Hulin, S. Kojima, E. Loyez, J.-R. Marquès, A. Morace, P. Nicolaï, M. Roth, S. Sakata, G. Schaumann, F. Serres, J. Serval, V. T. Tikhonchuk, N. Woolsey, and Z. Zhang, "Guiding of relativistic electron beams in dense matter by laser-driven magnetostatic fields," *Nature Communications*, vol. 9, p. 102, Jan 2018.
- [5] A. Bose, J. Peebles, C. A. Walsh, J. A. Frenje, N. V. Kabadi, P. J. Adrian, G. D. Sutcliffe, M. Gatu Johnson, C. A. Frank, J. R. Davies, R. Betti, V. Y. Glebov, F. J. Marshall, S. P. Regan, C. Stoeckl, E. M. Campbell, H. Sio, J. Moody, A. Crilly, B. D. Appelbe, J. P. Chittenden, S. Atzeni, F. Barbato, A. Forte, C. K. Li, F. H. Seguin, and R. D. Petrasso, "Effect of strongly magnetized electrons and ions on heat flow and symmetry of inertial fusion implosions," *Phys. Rev. Lett.*, vol. 128, p. 195002, May 2022.
- [6] C. N. Danson, C. Haefner, J. Bromage, T. Butcher, J.-C. F. Chanteloup, E. A. Chowd-

- hury, A. Galvanauskas, L. A. Gizzi, J. Hein, D. I. Hillier, and et al., “Petawatt and exawatt class lasers worldwide,” *High Power Laser Science and Engineering*, vol. 7, p. e54, 2019.
- [7] Z. Li, Y. Leng, and R. Li, “Further development of the short-pulse petawatt laser: Trends, technologies, and bottlenecks,” *Laser & Photonics Reviews*, vol. n/a, no. n/a, p. 2100705, 2022.
- [8] J. Zhu, J. Zhu, X. Li, B. Zhu, W. Ma, X. Lu, W. Fan, Z. Liu, S. Zhou, G. Xu, and et al., “Status and development of high-power laser facilities at the nlhplp,” *High Power Laser Science and Engineering*, vol. 6, p. e55, 2018.
- [9] J. Kawanaka, N. Miyanaga, H. Azechi, T. Kanabe, T. Jitsuno, K. Kondo, Y. Fujimoto, N. Morio, S. Matsuo, Y. Kawakami, R. Mizoguchi, K. Tauchi, M. Yano, S. Kudo, and Y. Ogura, “3.1-kj chirped-pulse power amplification in the lfex laser,” *Journal of Physics: Conference Series*, vol. 112, p. 032006, may 2008.
- [10] J. K. Crane, G. Tietbohl, P. Arnold, E. S. Bliss, C. Boley, G. Britten, G. Brunton, W. Clark, J. W. Dawson, S. Fochs, R. Hackel, C. Haefner, J. Halpin, J. Heebner, M. Henesian, M. Hermann, J. Hernandez, V. Kanz, B. McHale, J. B. McLeod, H. Nguyen, H. Phan, M. Rushford, B. Shaw, M. Shverdin, R. Sigurdsson, R. Speck, C. Stolz, D. Trummer, J. Wolfe, J. N. Wong, G. C. Siders, and C. P. J. Barty, “Progress on converting a nif quad to eight, petawatt beams for advanced radiography,” *Journal of Physics: Conference Series*, vol. 244, p. 032003, aug 2010.
- [11] D. Batani, M. Koenig, J. L. Miquel, J. E. Ducret, E. d’Humieres, S. Hulin, J. Caron, J. L. Feugeas, P. Nicolai, V. Tikhonchuk, L. Serani, N. Blanchot, D. Raffestin, I. Thfoin-Lantuejoul, B. Rosse, C. Reverdin, A. Duval, F. Lanieste, A. Chancé, D. Dubreuil, B. Gastineau, J. C. Guillard, F. Harrault, D. Leboeuf, J.-M. L. Ster, C. Pès, J.-C. Toussaint, X. Leboeuf, L. Lecherbourg, C. I. Szabo, J.-L. Dubois, and F. Lubrano-Lavaderci, “Development of the petawatt aquitaine laser system and new perspectives in physics,” *Physica Scripta*, vol. 2014, p. 014016, may 2014.
- [12] M. G. Haines, “Generation of an axial magnetic field from photon spin,” *Physical Review Letters*, vol. 87, p. 135005, Sep 2001.
- [13] Z. M. Sheng and J. Meyer-ter Vehn, “Inverse faraday effect and propagation of circularly polarized intense laser beams in plasmas,” *Physical Review E*, vol. 54, pp. 1833–1842, Aug 1996.
- [14] Z. Najmudin, M. Tatarakis, A. Pukhov, E. L. Clark, R. J. Clarke, A. E. Dangor, J. Faure, V. Malka, D. Neely, M. I. K. Santala, and K. Krushelnick, “Measurements of the inverse faraday effect from relativistic laser interactions with an underdense plasma,” *Physical Review Letters*, vol. 87, p. 215004, Nov 2001.
- [15] S. Ali, J. R. Davies, and J. T. Mendonca, “Inverse faraday effect with linearly polarized laser pulses,” *Physical Review Letters*, vol. 105, p. 035001, Jul 2010.
- [16] Y. Shi, J. Vieira, R. M. G. M. Trines, R. Bingham, B. F. Shen, and R. J. Kingham, “Magnetic field generation in plasma waves driven by co-propagating intense twisted lasers,” *Phys. Rev. Lett.*, vol. 121, p. 145002, Oct 2018.
- [17] J. Vieira, J. T. Mendonça, and F. Quéré, “Optical control of the topology of laser-plasma accelerators,” *Phys. Rev. Lett.*, vol. 121, p. 054801, Jul 2018.
- [18] R. Nuter, P. Korneev, I. Thiele, and V. Tikhonchuk, “Plasma solenoid driven by a laser beam carrying an orbital angular momentum,” *Physical Review E*, vol. 98, p. 033211, Sep 2018.
- [19] S. Sakata, S. Lee, H. Morita, T. Johzaki, H. Sawada, Y. Iwasa, K. Matsuo, K. F. F. Law, A. Yao, M. Hata, A. Sunahara, S. Kojima, Y. Abe, H. Kishimoto, A. Syuhada, T. Shiroto, A. Morace, A. Yogo, N. Iwata, M. Nakai, H. Sakagami, T. Ozaki, K. Yamanoi, T. Norimatsu, Y. Nakata, S. Tokita, N. Miyanaga, J. Kawanaka, H. Shiraga, K. Mima, H. Nishimura, M. Bailly-Grandvaux, J. J. Santos, H. Nagatomo, H. Azechi, R. Kodama, Y. Arikawa, Y. Sentoku, and S. Fujioka, “Magnetized fast isochoric laser heating for efficient creation of ultra-high-energy-density states,” *Nature communications*, vol. 9, pp. 3937–3937, Sep 2018. 30258053[pmid].
- [20] I. V. Kochetkov, N. D. Bukharskii, M. Ehret, Y. Abe, K. F. F. Law, V. Ospina-Bohorquez, J. J. Santos, S. Fujioka, G. Schaumann, B. Zielbauer, A. Kuznetsov, and P. Korneev, “Neural network analysis of quasistationary magnetic fields in microcoils driven by short laser pulses,” *Scientific Reports*, vol. 12, p. 13734, Aug 2022.
- [21] H. Morita and S. Fujioka, “Generation, measurement, and modeling of strong magnetic fields generated by laser-driven micro coils,” *Reviews of Modern Plasma Physics*, vol. 7, p. 13, Feb 2023.

- [22] T. Pisarczyk, O. Renner, R. Dudzak, T. Chodukowski, Z. Rusiniak, J. Dostal, M. Krupka, D. Klir, J. J. Domański, J. Krasa, S. Singh, J. Cikhardt, D. Batani, J. J. Santos, T. Burian, M. Ehret, P. Gajdos, A. Zaras-Szydłowska, M. Rosinski, P. Tchorz, M. Kustos, C. Vlachos, V. Ospina-Bohorquez, S. Jelinek, G. Kocourkova, S. Agrawal, S. Borodziuk, M. Krus, and L. Juha, “Strongly magnetized plasma produced by interaction of nanosecond kJ-class laser with snail targets,” Plasma Physics and Controlled Fusion, 2023.
- [23] M. Murakami, J. J. Honrubia, K. Weichman, A. V. Arefiev, and S. V. Bulanov, “Generation of megatesla magnetic fields by intense-laser-driven microtube implosions,” Scientific Reports, vol. 10, p. 16653, Oct 2020.
- [24] Y. Shi, K. Weichman, R. J. Kingham, and A. V. Arefiev, “Magnetic field generation in a laser-irradiated thin collisionless plasma target by return current electrons carrying orbital angular momentum,” New Journal of Physics, vol. 22, p. 073067, Jul 2020.
- [25] T. C. Wilson, Z.-M. Sheng, B. Eliasson, and P. McKenna, “Magnetic field amplification by high power lasers in underdense plasma,” Plasma Physics and Controlled Fusion, vol. 63, p. 084001, Jun 2021.
- [26] M.-A. H. Zosa, Y. J. Gu, and M. Murakami, “100-kt magnetic field generation using paisley targets by femtosecond laser-plasma interactions,” Applied Physics Letters, vol. 120, no. 13, p. 132403, 2022.
- [27] J. R. Davies, A. R. Bell, and M. Tatarakis, “Magnetic focusing and trapping of high-intensity laser-generated fast electrons at the rear of solid targets,” Physical Review E, vol. 59, pp. 6032–6036, May 1999.
- [28] A. Robinson, D. Strozzi, J. Davies, L. Gremillet, J. Honrubia, T. Johzaki, R. Kingham, M. Sherlock, and A. Solodov, “Theory of fast electron transport for fast ignition,” Nuclear Fusion, vol. 54, p. 054003, Apr 2014.
- [29] L. G. Huang, H. Takabe, and T. E. Cowan, “Maximizing magnetic field generation in high power laser–solid interactions,” High Power Laser Science and Engineering, vol. 7, p. e22, 2019.
- [30] J. M. Tian, H. B. Cai, W. S. Zhang, E. H. Zhang, B. Du, and S. P. Zhu, “Generation mechanism of 100 mg magnetic fields in the interaction of ultra-intense laser pulse with nanostructured target,” High Power Laser Science and Engineering, vol. 8, p. e16, 2020.
- [31] L. Gorbunov, P. Mora, and T. M. Antonsen, Jr., “Magnetic field of a plasma wake driven by a laser pulse,” Physical Review Letters, vol. 76, pp. 2495–2498, Apr 1996.
- [32] Z. M. Sheng, J. Meyer-ter Vehn, and A. Pukhov, “Analytic and numerical study of magnetic fields in the plasma wake of an intense laser pulse,” Physics of Plasmas, vol. 5, no. 10, pp. 3764–3773, 1998.
- [33] A. R. Bell and R. J. Kingham, “Resistive collimation of electron beams in laser-produced plasmas,” Phys. Rev. Lett., vol. 91, p. 035003, Jul 2003.
- [34] J. Zheng, K. A. Tanaka, T. Sato, T. Yabuuchi, T. Kurahashi, Y. Kitagawa, R. Kodama, T. Norimatsu, and T. Yamanaka, “Study of hot electrons by measurement of optical emission from the rear surface of a metallic foil irradiated with ultraintense laser pulse,” Phys. Rev. Lett., vol. 92, p. 165001, Apr 2004.
- [35] V. Kaymak, A. Pukhov, V. N. Shlyaptsev, and J. J. Rocca, “Nanoscale ultradense z-pinch formation from laser-irradiated nanowire arrays,” Phys. Rev. Lett., vol. 117, p. 035004, Jul 2016.
- [36] F. Zhang, H. B. Cai, W. M. Zhou, Z. S. Dai, L. Q. Shan, H. Xu, J. B. Chen, F. J. Ge, Q. Tang, W. S. Zhang, L. Wei, D. X. Liu, J. F. Gu, H. B. Du, B. Bi, S. Z. Wu, J. Li, F. Lu, H. Zhang, B. Zhang, M. Q. He, M. H. Yu, Z. H. Yang, W. W. Wang, H. S. Zhang, B. Cui, L. Yang, J. F. Wu, W. Qi, L. H. Cao, Z. Li, H. J. Liu, Y. M. Yang, G. L. Ren, C. Tian, Z. Q. Yuan, W. D. Zheng, L. F. Cao, C. T. Zhou, S. Y. Zou, Y. Q. Gu, K. Du, Y. K. Ding, B. H. Zhang, S. P. Zhu, W. Y. Zhang, and X. T. He, “Enhanced energy coupling for indirect-drive fast-ignition fusion targets,” Nature Physics, vol. 16, pp. 810–814, Jul 2020.
- [37] W.-M. Wang, P. Gibbon, Z.-M. Sheng, and Y.-T. Li, “Magnetically assisted fast ignition,” Phys. Rev. Lett., vol. 114, p. 015001, Jan 2015.
- [38] A. Arefiev, T. Toncian, and G. Fiksel, “Enhanced proton acceleration in an applied longitudinal magnetic field,” New Journal of Physics, vol. 18, p. 105011, Oct 2016.
- [39] K. Weichman, A. P. L. Robinson, M. Murakami, J. J. Santos, S. Fujioka, T. Toncian, J. P. Palastro, and A. V. Arefiev, “Progress in relativistic laser–plasma interaction with kilotesla-level

- applied magnetic fields,” Physics of Plasmas, vol. 29, no. 5, p. 053104, 2022.
- [40] D. Lai, “Matter in strong magnetic fields,” Rev. Mod. Phys., vol. 73, pp. 629–662, Aug 2001.
- [41] F.-L. Wang, X.-X. Pei, B. Han, H.-G. Wei, D.-W. Yuan, G.-Y. Liang, G. Zhao, J.-Y. Zhong, Z. Zhang, B.-J. Zhu, and et al., “Laboratory astrophysics with laser-driven strong magnetic fields in china,” High Power Laser Science and Engineering, vol. 4, p. e27, 2016.
- [42] A. Morace, N. Iwata, Y. Sentoku, K. Mima, Y. Arikawa, A. Yogo, A. Andreev, S. Tosaki, X. Vaisseau, Y. Abe, S. Kojima, S. Sakata, M. Hata, S. Lee, K. Matsuo, N. Kamitsukasa, T. Norimatsu, J. Kawanaka, S. Tokita, N. Miyanaga, H. Shiraga, Y. Sakawa, M. Nakai, H. Nishimura, H. Azechi, S. Fujioka, and R. Kodama, “Enhancing laser beam performance by interfering intense laser beamlets,” Nature Communications, vol. 10, p. 2995, Jul 2019.
- [43] C. Hernandez-Gomez, S. P. Blake, O. Chekhlov, R. J. Clarke, A. M. Dunne, M. Galimberti, S. Hancock, R. Heathcote, P. Holligan, A. Lyachev, P. Matousek, I. O. Musgrave, D. Neely, P. A. Norreys, I. Ross, Y. Tang, T. B. Winstone, B. E. Wyborn, and J. Collier, “The vulcan 10 pw project,” Journal of Physics: Conference Series, vol. 244, p. 032006, aug 2010.
- [44] A. M. Beloborodov, “Scattering of ultrastrong electromagnetic waves by magnetized particles,” Phys. Rev. Lett., vol. 128, p. 255003, Jun 2022.
- [45] H. Takabe and Y. Kuramitsu, “Recent progress of laboratory astrophysics with intense lasers,” High Power Laser Science and Engineering, vol. 9, p. e49, 2021.
- [46] F. Tamburini, B. Thidé, G. Molina-Terriza, and G. Anzolin, “Twisting of light around rotating black holes,” Nature Physics, vol. 7, pp. 195–197, Mar 2011.
- [47] F. Tamburini, B. Thidé, and M. Della Valle, “Measurement of the spin of the M87 black hole from its observed twisted light,” Monthly Notices of the Royal Astronomical Society: Letters, vol. 492, pp. L22–L27, 11 2019.
- [48] K. Y. Bliokh, F. J. Rodríguez-Fortuño, F. Nori, and A. V. Zayats, “Spin-orbit interactions of light,” Nature Photonics, vol. 9, pp. 796–808, Dec 2015.
- [49] C. Liu, B. Shen, X. Zhang, Y. Shi, L. Ji, W. Wang, L. Yi, L. Zhang, T. Xu, Z. Pei, and Z. Xu, “Generation of gamma-ray beam with orbital angular momentum in the qed regime,” Physics of Plasmas, vol. 23, no. 9, p. 093120, 2016.
- [50] Y.-Y. Chen, J.-X. Li, K. Z. Hatsagortsyan, and C. H. Keitel, “ γ -ray beams with large orbital angular momentum via nonlinear compton scattering with radiation reaction,” Phys. Rev. Lett., vol. 121, p. 074801, Aug 2018.
- [51] Y.-Y. Chen, K. Z. Hatsagortsyan, and C. H. Keitel, “Generation of twisted γ -ray radiation by nonlinear thomson scattering of twisted light,” Matter and Radiation at Extremes, vol. 4, no. 2, p. 024401, 2019.
- [52] T. Arber, K. Bennett, C. Brady, A. Lawrence-Douglas, M. Ramsay, N. Sircombe, P. Gillies, R. Evans, H. Schmitz, A. Bell, and C. Ridgers, “Contemporary particle-in-cell approach to laser-plasma modelling,” Plasma Physics and Controlled Fusion, vol. 57, no. 11, p. 113001, 2015.
- [53] S. Jiang, L. L. Ji, H. Audesirk, K. M. George, J. Snyder, A. Krygier, P. Poole, C. Willis, R. Daskalova, E. Chowdhury, N. S. Lewis, D. W. Schumacher, A. Pukhov, R. R. Freeman, and K. U. Akli, “Microengineering laser plasma interactions at relativistic intensities,” Phys. Rev. Lett., vol. 116, p. 085002, Feb 2016.
- [54] D. Wu, W. Yu, Z. M. Sheng, S. Fritzsche, and X. T. He, “Uniform warm dense matter formed by direct laser heating in the presence of external magnetic fields,” Phys. Rev. E, vol. 101, p. 051202, May 2020.
- [55] K. Li and W. Yu, “Parametric dependence of collisional heating of highly magnetized overdense plasma by (far-)infrared lasers,” High Power Laser Science and Engineering, vol. 10, p. 04000e23, 4 2022.
- [56] A. Longman and R. Fedosejevs, “Kilo-tesla axial magnetic field generation with high intensity spin and orbital angular momentum beams,” Phys. Rev. Research, vol. 3, p. 043180, Dec 2021.
- [57] J. D. Jackson, Electrodynamics. Wiley Online Library, 1975.
- [58] F. Brunel, “Anomalous absorption of high intensity subpicosecond laser pulses,” The Physics of Fluids, vol. 31, no. 9, pp. 2714–2719, 1988.

- [59] M. C. Levy, S. C. Wilks, M. Tabak, S. B. Libby, and M. G. Baring, “Petawatt laser absorption bounded,” *Nature Communications*, vol. 5, p. 4149, Jun 2014.
- [60] A. Grassi, M. Grech, F. Amiranoff, A. Macchi, and C. Riconda, “Radiation-pressure-driven ion weibel instability and collisionless shocks,” *Phys. Rev. E*, vol. 96, p. 033204, Sep 2017.
- [61] W. Yao, M. Nakatsutsumi, S. Buffechoux, P. Antici, M. Borghesi, S. N. Chen, E. d’Humières, L. Gremillet, R. Heathcote, V. Horný, M. N. Quinn, L. Romagnani, R. Royle, G. Sarri, Y. Sentoku, H.-P. Schlenvoigt, T. Toncian, O. Tresca, L. Vassura, O. Willi, and J. Fuchs, “Optimizing the laser coupling, matter heating, and particle acceleration from solids by using multiplexed ultraintense lasers,” 2022. arXiv:2208.06272.